Influence of Band Width on the Scattered Ion Yield Spectra of a He^+ ion by Resonant or Quasi-Resonant Charge Exchange Neutralization

Shin-ichiro KONDO

Department of Materials Science and Engineering, Nagasaki University, Nagasaki 852-8521

(Received)

The influence of the band structure, especially the bandwidth, on the scattered ion yield spectra of a He^+ ion by the resonant or quasi-resonant neutralization was theoretically examined using quantum rate equations. When calculating the scattered ion yield spectra of He^+ to simulate the experimental data, we observed that the band structure, especially the bandwidth, had a strong influence on the spectra at relatively low incident He^+ ion energies of less than several hundred eV. Through many simulations, it was determined that theoretical calculations that include bandwidth calculation can simulate or reproduce the experimentally observed spectra of He^+-In, He^+-Ga, and He^+-Sn systems. In contrast, simulations not including bandwidth simulation could neither reproduce nor account for such spectra. Furthermore, the calculated ion survival probability (ISP) at low incident ion energies tended to decrease with increasing bandwidth. This decrease in ISP probably corresponds to the relatively small scattered ion yield usually observed at low incident ion energies. Theoretically, such a decrease indicates that a He^+ ion with a low incident energy can be easily neutralized on the surface when the bandwidth is large.

KEYWORDS: resonant neutralization, He^+ ion, bandwidth, ion survival probability, ion scattering spectrometry, Heisenberg equations of motion

1. Introduction

Ion scattering spectrometry (ISS) [1-7] is an important method of surface analysis, together with secondary ion mass spectroscopy (SIMS)[8-12], electron or photo-stimulated desorption (ESD, PSD) study [13-18], and ion neutralization spectroscopy (INS)[19-22]. Through measurements of the intensity, kinetic energy, and angular distribution of surviving backscattered ions as functions of the incident energy and direction of the ions, ISS provides useful information related to surface properties, such as composition, structure, location of absorbed atoms, and electronic states. ISS is also a powerful and useful tool for characterizing surfaces through analysis of the scattering of low-energy ions at solid surfaces. However, some dynamic aspects associated with time-dependent quantum effects have not been completely resolved, despite extensive theoretical and experimental efforts.

One of the problems that has not been completely resolved or analyzed is resonant or quasi-resonant charge exchange on a surface. This process includes resonance tunneling (RT) and energy-level crossing (EC), both of which are strongly associated with quantum dynamics. Therefore, it is important to investigate this problem theoretically.

When an empty energy level of an ion is close to the continuum of electronic states of a metal solid surface, a resonant or quasi-resonant charge process can take place, and neutralization occurs as a result of the charge transfer between the ion and the metal surface. However, such a neutralization process has been considered a specific case[19,23-24] in comparison with the Auger neutralization process. However, a strong dependence of the Ne^+ ion yield in scattering from a metal surface on the metal work function ϕ has recently been observed[25-26]. Therefore, the resonant or quasi-resonant

charge exchange process is considered not to be very specific but rather to be the dominant neutralization pathway, as opposed to the Auger process, if the empty energy level of the ion is close to the energy level of the metal.

For neutralization resulting from the resonant or quasi-resonant charge exchange process, we can refer to the neutralization of He^+ ions occurring on a metal surface. This process has been known to exhibit oscillations with increasing incident ion energy. The origin of this oscillatory behavior can be explained by the quantum interference caused by the difference between the phases of the two states (the state of an ion approaching the target atom and the state of an ion retreating from the target atom). However, a detailed evaluation of the electronic structure of the metal surface remains to be discussed, even though such a quantum oscillation would include information related to the electronic structure of the metal surface. Accordingly, further investigation of these neutralization processes is essential to understanding the surface dynamics and surface electronic structure in detail.

The neutralization of a rare-gas ion on a metal surface and the resulting oscillation were first experimentally observed in the He^+-Pb, He^+-Ge, He^+-Bi, and He^+-In systems by Erickson and Smith[27]. On the basis of the analysis by Tolk and cowarkers[28-29], the angular dependence of the backscattered oscillatory intensity implied a near-resonant charge–exchange process, i.e., a quasi-resonant process. Similar oscillations were observed in He^+-Ga and He^+-Sn systems[30]. Furthermore, from experiments related to the He^+-Pb system by Zartner *et al.*[31], the ion yield of He^+ scattered from atomic Pb (Pb beam) showed oscillation as a function of the energy of the incident ion, indicating that the atomic nature has a strong effect on the quasi-resonant charge exchange process. However, it should be

noted that the scattered He^+ ion yield from epitaxial HgCdTe on CdTe showed oscillation similar to that observed in the He^+-Sn system, but that the scattered He^+ ion yield from Te showed no oscillation, i.e., a smooth curve[32]. Such an oscillation from epitaxial HgCdTe on CdTe could be interpreted as the appearance of a quasi-resonant state, caused by a change in Te energy level. Consequently, the detailed conditions leading to quasi-resonant exchange remain to be elucidated. Additionally, inelastic energy losses for the He^+-Pb[33] and He^+-Sn[34] systems were investigated and showed good agreement with the Oen-Robinson model [35].

Concerning the theoretical analysis of data of such experiments with rare-gas ion neutralization on metal or metallic compound surfaces, as described in the previous paragraph, Tully first discussed the quantum mechanics of the He^+-Cd, He^+-Ga, He^+-Pb, He^+-In, He^+-Sn, and He^+-Sb systems[36], using an approach based on solving the time-dependent Schrödinger equation $H\Psi = i\hbar\partial\Psi/\partial t$. In this calculation, the total wave function Ψ was expanded into the summation of the terms of the basis functions, so that differential equations consisting of expansion coefficients could be numerically solved. However, the obtained solutions did not agree well with experimental observations. On the basis of the explanation by Tully, the discrepancies between the theoretical and experimental results were due to the very approximate nature of the interaction potential used in their calculations. Subsequently, Easa and Modinos.[37] extended Tully's semi-empirical theory using a Born-Mayer-type interaction potential between the projectile and target atoms. In their study[37], they set the two states $|0\rangle$ and $|A\rangle$, where $|A\rangle$ is the configuration of the occupied valence level of the ion (projectile) and all occupied energy levels of the metal except the inner vacant *d*-level and $|0\rangle$

represents the empty valence level of the ion (projectile) and all occupied energy levels of the metal. On the basis of the numerical analysis of several differential equations using the expansion coefficients obtained by substituting the two states with the expansion coefficients into the time-dependent Schrödinger equation $H\Psi = i\hbar\partial\Psi/\partial t$, they evaluated the ion survival probability (ISP). The obtained results of ion yield spectra greatly improved the agreement with the experimental data, and the theoretically evaluated ISPs were similar to those obtained experimentally. However, the description of the $|0\rangle$ and $|A\rangle$ states neglected many electron states over time $-\infty < t < \infty$. In addition, Vitanov and Panev generalize the Demkov formula in near-resonant charge transfer on the basis of WKB approximation, attempting to explain the K^+-Rb and Li+-Na systems (oscillating structures as charge exchange at quasi-resonance) with the use of the two time-dependent states (initial and final states)[38]. However, many quantum states mixing with the ion and surface band electrons should be considered especially when ion and surface are very close.

The Keldysh formalism has regularly been used generally for such calculations of nonequilibrium time-dependent states[39]. This method is very effective and has been applied to many fields of analysis of nonsteady states, such as quantum dots, point-conduct tunnel junctions, and spintronic devices and surfaces. In surface physics, the time-resolved two-photon photoemission from Cu(100)[40], the formation of H^- ions from collision with a Si surface[41], and the scanning tunneling microscopy (STM) tunneling current for ultrathin Pb on Si(111) substrates [42] have been analyzed using this method. Although the merits of Green's function methods have been discussed and actually been applied in various fields, showing good agreement with experimental data, calculations

for such complicated systems require considerable time as well as complex analytical schemes, such as the evaluation of self-energy and Dyson's equation.

Consequently, to reduce the discrepancies between the calculation and the experiment, and to investigate the electronic states of metal surfaces in detail through comparison of quasi-resonant experimental data for He^+ neutralization on various metal surfaces, we applied a novel numerical approach. We employed quantum rate equations composed of differential equations [43] to solve these problems, with emphasis on many-electron effects. Our proposed method is very simple, with no need of complex analytical schemes derived from Dyson's equations.

This study is an extension of an earlier study that showed the quantum rate equation and its application to various systems [43]. In the earlier study, we derived quantum rate equations on the basis of the Heisenberg equation of motion. Numerical results obtained by solving the quantum rate equations showed good agreement with the theoretical conclusion, as analyzed and discussed previously[44]. Furthermore, we applied this method to the neutralization process under an impurity potential and obtained interesting results [43].

On the basis of our proposed method, it is possible to evaluate $n_{aa}(\infty)$ (number of electrons occupying the He^+ ion orbital at $t = \infty$) directly, without any approximations, even when new perturbative Hamiltonians, such as an impurity potential, are introduced into the nonperturbative Hamiltonian. Additionally, complex calculations including time-dependent terms can be performed without any integral procedures. Since our theoretical approach is based on the transformation of the Heisenberg operator (Q-number) into a *c*-number, the proposed method can be easily applied to the

direct calculation of neutralization probability, i.e., $n_{aa}(\infty)$, even when the Hamiltonian includes a new perturbative Hamiltonian or complex time-dependent terms. Furthermore, using proposed method, it is be possible to evaluate the band structures such as bandwidth and density of states(DOS) and many parameters by comparison with experimental data.

In this study, therefore, to investigate the effect of $3d$ –or $4d$ bands electrons on the resonant charge transfer process of a rare-gas ion and to estimate these band properties from the ISS measurements, we discuss the application of our method to the neutralization of He^+ ions, on various metal surfaces, with emphasis on many-electron effects. Many transition quantum states are thought to appear and disappear as an ion approaches a surface. Therefore, calculations including precise information related not only to the target atom, but also to its surroundings, are essential and calculations including many-electron terms are required. In addition, it should be noticed that although oscillating structures as charge exchange structures at quasi resonance have been theoretically analyzed by several authors, their band properties have never been investigated through comparison with experimentally obtained ISS data. In §2, we briefly discuss the theoretical framework on the basis of the Heisenberg equations of motion and derive simultaneous differential equations. In §3, numerical results obtained by applying our method to the neutralization of He^+ ions on a metal surface are illustrated in comparison with experimental data, with emphasis on the band structure of the metal surface. Finally, in §4, we conclude with a discussion of the remaining problems and future research.

2. Quantum Rate Equations

As discussed previously[43], quantum rate equations were derived from the Heisenberg equations of motion. On the basis of the Heisenberg equations of motion, the time dependence of the operator $\hat{a}_i^+(t)$ is given by

$$i\hbar \frac{\partial}{\partial t}\hat{a}_i^+(t) = \left[\hat{a}_i^+(t), \hat{H}\right] , \tag{1}$$

where the operator $\hat{a}_i^+(t)$ is in the Heisenberg representation. By using eq. (1), the differentiation of $\hat{a}_i^+(t)\hat{a}_j(t)$ can be expressed as

$$\frac{\partial}{\partial t}\hat{a}_i^+(t)\hat{a}_j(t) = \frac{1}{i\hbar}\left[a_i^+(t), \hat{H}\right]\hat{a}_j(t) + \frac{1}{i\hbar}\hat{a}_i^+(t)\left[\hat{a}_j(t), \hat{H}\right] . \tag{2}$$

By taking the expectation value of each term, we obtain the following differential equation, i.e., the quantum rate equation,

$$\frac{d}{dt} < \hat{a}_i^+(t)\hat{a}_j(t) > = \frac{1}{i\hbar} < \left[a_i^+(t), \hat{H}\right]\hat{a}_j(t) > + \frac{1}{i\hbar} < \hat{a}_i^+(t)\left[\hat{a}_j(t), \hat{H}\right] > , \tag{3}$$

where <***> denotes the quantum-mechanical expectation value.

3. Application of Quantum Rate Equations to Analysis of Resonant or Quasi-Resonant Systems

Let us apply eq. (3) to the analysis of the resonant or quasi-resonant charge exchange process, in which a singly charged rare-gas ion, such as He^+, approaches a metal surface, collides with the surface, and then moves away from it, thus interacting with the inner *d*-levels of the target atoms. Initially, to simplify the discussion of the resonant or quasi-resonant charge exchange process, we assume that the target atom *d*-level has only one energy level, E_d, with no band structure formation (a localized *d* state model). The resulting spinless Anderson-Newns Hamiltonians are given as

$$\hat{H} = \hat{H}_0 + \hat{H}', \tag{4}$$

$$\hat{H}_0 = E_d \hat{C}_d^+ \hat{C}_d + E_a(z) \hat{C}_a^+ \hat{C}_a, \tag{5}$$

$$\hat{H}' = V_{ad}(z) \hat{C}_a^+ \hat{C}_d + V_{da}(z) \hat{C}_d^+ \hat{C}_a . \tag{6}$$

In the above equations, E_d is the inner *d*-level of the target atom, $\hat{C}_d^+$ and $\hat{C}_d$ are the creation and annihilation operators of the inner *d*-level of the target atom, respectively, $E_a(z)$ denotes the energy level of the ion that usually depends on the surface-ion distance *z*, $\hat{C}_a^+$ and $\hat{C}_a$ are the creation and annihilation operators of the state of the ion, respectively, and $V_{ad}(z)$ is an electron transfer matrix element from the inner *d*-level of the target atom to the state of the ion that is expressed as a function of the surface-ion distance *z*. Since *z* can be expressed as a function of time, we hereafter use $E_a(t)$, $V_{ad}(t)$, and $V_{da}(t)$ instead of $E_a(z)$, $V_{ad}(z)$, and $V_{da}(z)$.

From eqs. (4)-(6),

$$[\hat{C}_a(t), \hat{H}] = E_a(t) \hat{C}_a(t) + V_{ad}(t) \hat{C}_d(t), \tag{7}$$

$$[\hat{C}_d(t), \hat{H}] = E_d \hat{C}_d(t) + V_{da}(t) \hat{C}_a(t) . \tag{8}$$

Combining eqs. (7) and (8) with eq. (3), we obtain the following quantum rate equations:

$$\frac{d}{dt} n_{aa}(t) = \frac{\mathrm{i}}{\hbar} [V_{da}(t) n_{da}(t) - V_{ad}(t) n_{ad}(t)], \tag{9}$$

$$\frac{d}{dt} n_{da}(t) = \frac{\mathrm{i}}{\hbar} [(E_d - E_a(t)) n_{da}(t) + V_{ad}(t)(n_{aa}(t) - n_{dd}(t))], \tag{10}$$

$$\frac{d}{dt} n_{dd}(t) = \frac{\mathrm{i}}{\hbar} (V_{ad}(t) n_{ad}(t) - V_{da}(t) n_{da}(t)). \tag{11}$$

In the above equations, we define

$$n_{ij}(t) \equiv <\hat{C}_i^+(t)\hat{C}_j(t)>, \tag{12}$$

and $n_{ji}(t)$ is obtained from the relation $n_{ji}(t) = (n_{ij}(t))^*$.

From eqs. (9) and (11),

$$\frac{d}{dt}n_{aa}(t) + \frac{d}{dt}n_{dd}(t) = 0;$$

Consequently, we obtain the following conservative equation for the total number of electrons:

$$n_{aa}(t) + n_{dd}(t) = \text{const} = n_{aa}(-\infty) + n_{dd}(-\infty) \equiv N(-\infty). \tag{13}$$

Equation (13) indicates that the sum of the number of electrons occupying the inner *d*-level of the target atom and the state of the ion remains constant over time, i.e., $-\infty < t < \infty$. Furthermore, using eq. (13) and assuming $\text{Im}(V_{ad}(t)) = \text{Im}(V_{da}(t)) = 0$ and $\text{Re}(V_{ad}(t)) = \text{Re}(V_{da}(t)) = V(t)$, we obtain the differential-integrate equation for determining $n_{aa}(t)$:

$$\frac{d}{dt}n_{aa}(t) = 2\left(\frac{i}{\hbar}\right)^2 V(t)\int_{-\infty}^{t} d\tau V(\tau)(2n_{aa}(\tau) - N(-\infty))\cos[\frac{1}{\hbar}\int_{\tau}^{t}(E_d - E_a(x))dx] \ . \tag{14}$$

Assuming $n_{aa}(t) = \text{const}$ to be the particular solution of the above equation, we obtain the following relation because $dn_{aa}(t)/dt = 0$ for $-\infty < t < \infty$:

$$2n_{aa}(-\infty) - N(-\infty) = n_{aa}(-\infty) - n_{dd}(-\infty) = 0. \tag{15}$$

Accordingly, we can conclude that $n_{aa}(t)$ retains a constant $n_{aa}(-\infty)$ if the initial condition is $N_{aa}(-\infty) = 0$ or 2. This result indicates that no electron transfer occurs between the ion and the target atom if both the ion state and the inner *d*-level are occupied or empty at $t = -\infty$. Furthermore, when $E_a(t) = E_d$, eq. (14) can be simplified and a second-order linear differential equation with respect to $n_{aa}(t)$ can be deduced:

$$\ddot{n}_{aa}(t) - \frac{\dot{V}(t)}{V(t)}\dot{n}_{aa}(t) - 2\left(\frac{i}{\hbar}\right)^2 V^2(t)(2n_{aa}(t) - N(-\infty)) = 0 . \quad (16)$$

In the above equation, $\dot{n}_{aa}(t) \equiv \frac{d}{dt} n_{aa}(t)$, $\dot{V}(t) \equiv \frac{d}{dt} V(t)$ and $\ddot{n}_{aa}(t) \equiv (\frac{d}{dt})^2 n_{aa}(t)$.

Figure 1 shows the time dependence of ISP, where ISP is defined as $1 - n_{aa}(\infty)$. We set $V(t) = V_0 \exp(-\zeta v^2 t^2)$ (v: ion velocity, ζ: positive constant) and $E_a(t) = E_d$. In the calculations, V_0, ζ, and v were 1.2 eV, 1.0 Å^{-2}, and 15 km/s, respectively. As shown in the figure, the ISP oscillated in the range of about $t \cong 0$, indicating that electrons frequently transferred between singly charged rare-gas ions and the inner *d*-level of the target atom in the vicinity of the surface. Because of the presence of the mixed region caused by the energy-level crossing between ions and target atoms, electrons were considered to move freely between the two potential states of R^+-M and R-M^+ (R: rare-gas, M: target atom) in an adiabatic manner[34]. Thus, oscillation such as that shown in Fig. 1 indicates the adiabatic electron transfer between two potential states.

Figure 2 shows the dependence of ISP on ion velocity. Although oscillations were observed, their period increased with increasing velocity. When the ion velocity is infinite, i.e., $v \to +\infty$, we can simplify eq. (16) by setting $V(t) = V_0 \exp(-\zeta v^2 t^2)$:

$$\ddot{n}_{aa}(t) + 2\zeta v^2 t\, \dot{n}_{aa}(t) \approx 0 . \quad (17)$$

Consequently, we obtain $\lim_{v\to\infty} n_{aa}(\infty) = n_{aa}(-\infty)$ from the relation $\ln\left|\dot{n}_{aa}(t)\right| + \zeta v^2 t^2 = C$ (C: an arbitrary integral constant) and the above equation. Furthermore, provided that $V(t)$ satisfies $\lim_{v\to\infty} V(t) = 0$, regardless of $V(t)$, we can derive the following equation from $\ddot{n}_{aa}(t)/\dot{n}_{aa}(t) - \dot{V}(t)/V(t) = 0$ in the limit $v \to +\infty$:

$$n_{aa}(t) = C_0 \int_{-\infty}^{t} V(\tau) d\tau + n_{aa}(-\infty), \text{ and } \lim_{v \to \infty} n_{aa}(\infty) = n_{aa}(-\infty), \tag{18}$$

where C_0 is an arbitrary integral constant. Equation (18) indicates that no electron transfer occurs between ions and the surface because there is insufficient time when the ion velocity is too high. Therefore, a rare-gas ion cannot be neutralized in the limit $v \to +\infty$. In other words, the ISP approaches unity with increasing ion velocity.

Let us consider the above point from the viewpoint of the charge exchange process with the accompanying energy-level crossing, which has been explored in the field of atomic and molecular collisions, with the well-known Landau-Zener model[45-47] being the most popular approach. On the basis of their formula, the one-way survival probability p of remaining in the initial state is expressed as

$$p = \exp\left(-\frac{2\pi \left| \widetilde{V} \right|^2}{\hbar v \Delta F} \right), \tag{19}$$

where $\widetilde{V}$ is the interaction matrix element, ΔF is the difference in slope between the two potential surfaces, and v is the velocity of the ion or atom. On the basis of the theoretical calculations by Bykhovskii *et al.*[48], the transition probability P from one state to another state, which included both the approach to and departure from the target, can be approximately expressed as follows, using the one-way survival probability p from eq. (19):

$$P \approx 2p(1-p). \tag{20}$$

The ISP, i.e., $1 - n_{aa}(\infty)$, can therefore be expressed as $1 - P \approx (1-p)^2 + p^2$. In the limit $v \to +\infty$,

$1-P \to 1$ because $p \to 1$ from eq. (19), which is consistent with our result that ISP approaches unity with increasing ion velocity.

Next, to investigate and interpret the various reports on resonant and quasi-resonant charge exchange processes, such as the experimentally observed He^+-Ga, He^+-Sn, and He^+-In systems[30,34], let us consider that $E_a(z)$, the energy level of the ion, has a time dependence as a result of the interaction between the target atom and the ion.

As the ion approaches the surface, the electrostatic attraction between the ion and its image potential in the surface has a dominant effect on the energy level of the ion, and the ion will experience a strong repulsion very close to the surface because of Pauli repulsion. Accordingly, the dependence of the ion energy level E_a on the surface-ion distance z can be expressed as follows in atomic units:

$$E_a = E_a(z) = \phi - I + \frac{1}{4(z - z_{im})}, \tag{21}$$

where ϕ, I, and z_{im} are the work function, ionization potential, and the location of the image potential (we take $z_m = -2a_B$ in the following calculations, a_B : Bohr radius), respectively. We set I = 24.58 eV, which is the first ionization potential of He[49]. In subsequent calculations, we assumed the Fermi level of solid to be E_F = 0.

Figure 3 shows the calculated relationship between ISP and the ion velocity v for work functions ϕ = 1, 3, and 5 eV. When calculating ISP, we assumed a binding energy of the target atom of 20 eV, which corresponds to the 4*d*-electron binding energy of In [50]. As shown in the figure, the

behavior of ISP is strongly dependent on ϕ. Frequent oscillations in the ISP were observed for ϕ = 3 eV, whereas ISP was monotonic and changed only gradually in the other cases.

Figure 4 shows the relationship between the ion-surface distance *z* and the energy level of the ion E_a. As shown in the figure, $E_a(z)$ crosses the binding energy of the target atoms at about *z* = 1 Å when ϕ = 3 eV. In contrast, there were no energy-level crossings between the energy level of the 4*d* inner core and the energy level of the ion for ϕ = 1 or 5 eV, which were lower and higher than the 4*d* inner level for ϕ = 1 and 5 eV, respectively.

As illustrated in the previous figure, when an ion (He ion) with ϕ = 3 eV approaches and then moves away from the surface, it passes into the mixing region formed by the energy level crossing of E_d = -20 eV. In other words, the ion passes into the mixing region twice. Therefore, the experimentally observed oscillations in the quasi-resonant charge exchange processes of the He^+-Sn, He^+-In, and He^+-Ga systems can be interpreted as the result of a phase difference between the two states of the ion and the surface, which independently evolve after first passing the crossing point, i.e., the mixing region during the approach[29,31-32,34,36-37]. Therefore, we can conclude that the oscillation observed in Fig. 3 is caused by a similar phase difference between the states of the ion and target atom. Furthermore, considering that the transition probability determines the spectra of the oscillations, as was experimentally observed, more detailed studies are recommended.

On the basis of the theoretical investigation using a time development operator by Tsuneyuki *et al.*[51], the transition probability $P(a \rightarrow b)$ from state *a* to state *b* in the resonance tunneling process can be expressed as a function of the scattering time *T*. Tsuneyuki et al's results indicated that

$P(a \to b) = 1 - \cos^2(V_0 T / \hbar)$ when the width of the Lorenzian band was reduced to 0 and the interaction $V(t)$ between the ion and the surface retained a constant V_0 for $0 \le t \le T$ and 0 for $t < 0$ or $t > T$. If we introduce the scattering length L, within which the interaction $V(t)$ switches on ($V(t) = V_0$) and $V(t)$ switches off ($V(t) = 0$) when $z > L$, then T is proportional to the inverse of the ion velocity v from the simple relation $2L = vT$. Transition probability can, therefore, be expressed as a function of the inverse of ion velocity, i.e., $1/v$, and $P(a \to b) = 1 - \cos^2(2LV_0 / \hbar v)$ with a constant period ($\pi\hbar / 2LV_0$).

To compare the above result with those of our proposed method, we apply the preceding conditions of $V(t) = V_0 \, (0 \le t \le T)$ and $0 (t < 0, t > T)$ to eq. (16) and obtain following differential equations:

$$\ddot{x}_{aa}(t) + 4{V_0}^2 x_{aa}(t) / \hbar^2 = 0 \quad (0 \le t \le T), \text{ and}$$

$$\ddot{x}_{aa}(t) = 0 \qquad (t < 0, t > T), \tag{22}$$

where we define $x_{aa}(t) \equiv 2n_{aa}(t) - N(-\infty)$. The solution of eq. (22) can be easily obtained under the initial conditions $n_{aa}(-\infty) = 0, n_{dd}(-\infty) = 1$ and $n_{aa}(\infty) = (1 - \cos(2V_0 T / \hbar)) / 2 = 1 - \cos^2(V_0 T / \hbar) = 1 - \cos^2(2LV_0 / v\hbar)$, which is the same as the transition probability result $P(a \to b)$ for the resonance tunneling process discussed in the previous paragraph. Since the above initial conditions indicate that no electrons occupy the ion level at $t = -\infty$, $n_{aa}(\infty)$ corresponds to the transition probability $P(a \to b)$. As shown above, it should be noted that the same calculation results are obtained, although the theoretical results of Tsuneyuki *et al.* [51] were significantly different from ours.

The above discussion indicates that $n_{aa}(\infty)$ is a simple cosine function with a constant period of $\pi\hbar/2LV_0$ when plotted against the inverse of ion velocity. Experimentally, it was also observed that the period of oscillation remained constant in the scattered He^+ ion yield from Sn when the data were plotted against the inverse of incident ion velocity[34]. In Kahn et al's He^+-Sn scattered ion yield experiment[34], the primary energies of the incident ion E_0 for several peaks in the ISS spectrum were roughly estimated to be about 434, 532, 670, 900, 1200, and 1620 eV. On the basis of the result of another experiment by Rusch and Erickson[30], we roughly determined E_0 for several peaks to be about 455, 579, 717, 924, 1255, and 1628 eV. Since the relationship between E_0 and ion velocity v satisfies $v^2 \propto E_0$, it follows that $1/v \propto \sqrt{1/E_0}$. Therefore, the calculated $\sqrt{1/E_0}$ values are 0.048, 0.044, 0.039, 0.033, 0.029, and 0.025 $eV^{-1/2}$ according to the experiments by Kahn *et al*. [34], and were 0.047, 0.042, 0.037, 0.033, 0.028, 0.025 $eV^{-1/2}$ for the experiments by Rusch and Erickson[30]. The period of quantum oscillation for the He^+-Sn system was evaluated to be approximately 0.004 $eV^{-1/2}$ in units of $\sqrt{1/E_0}$ in both experiments. Additionally, based on experiments by Rusch and Erickson [30], E_0 for several peaks was roughly estimated to be about 303, 386, 483, 566, 703, 883, 1145, and 1517 eV for the He^+-In system, and about 325, 450, 563, 738, 975, and 1413 eV for the He^+-Ga system. Therefore, the period of oscillation for the He^+-In and He^+-Ga systems were 0.004 and 0.005 $eV^{-1/2}$, respectively.

Figure 5 shows a plot of ISP from Fig. 3 for ϕ = 3 eV as a function of the inverse of ion velocity v, showing a constant period of oscillation. The estimated period is about 0.0097 s/km, which corresponds to 0.06 $eV^{-1/2}$, assuming $E_0 = 1/2\,MV^2$ (M: mass of a He atom). The theoretically

evaluated period is about ten times larger than the experimental one. The main reason for this discrepancy is that the theoretical oscillation occurs for relatively low incident energies, below approximately 280 eV, whereas the experimentally determined oscillation range was very wide, covering a range from approximately 300 to about 1500 eV.

Next, let us consider the interpretation of the measured scattered ion yield more precisely, using our proposed model. To account for the experimentally obtained data more qualitatively, and to simulate them more precisely, let us consider I_k for the measured elastically scattered ion yield from the *k*-th surface component**.** I_k can be given as a function of θ and E_0 (θ: laboratory scattering angle) [52]:

$$I_k = C_f N_k I_0 T D \Delta\Omega \sigma_k(E_0,\theta)\left[1 - P_n(E_0,\theta)\right]. \tag{23}$$

In the above equation, C_f, N_k, I_0, T, D, and $\Delta\Omega$ are coefficients containing the appropriate conversion factors, the concentration of the *k*-th component, the primary ion current, the analyzer transmissivity, the detector sensitivity, and the analyzer acceptance angle, respectively. $\sigma_k(E_0,\theta)$ and $P_n(E_0,\theta)$ are the differential scattering cross section for components consisting of the surface and the ion neutralization probability, respectively. Assuming $N_k = 1$ for the He^+-Ga, He^+-Sn, and He^+-In systems, and considering that C_f, I_0, T, D, and $\Delta\Omega$ can be attributed to the characteristics of the measurement system, such as the power of the ion gun and the analyzer capability, which have no physical properties, we can simplify the scattering ion yield I

$$I \propto \sigma(E_0,\theta)\left[1 - P_n(E_0,\theta)\right],$$

Because $P_n(E_0,\theta) \to n_{aa}(\infty)$, the experimentally measured scattering ion yield can be given as

$$I \propto \sigma(E_0, \theta)\left[1 - n_{aa}(\infty)\right]. \tag{24}$$

From classical scattering calculations based on the Bohr, Born-Mayer, and Thomas-Fermi interactions, it can be shown that the differential scattering cross section σ is a monotonically decreasing function of the primary ion energy E_0, with no dependence on the structure [53-54]. Additionally, the laboratory scattering angle θ was fixed at 90° in the experiments by Rusch and Erickson[30], while θ ranged from approximately 30 to 130° in the report by Kahn *et al*. [34] using their data for $\theta = 90^\circ$ for the analysis of the period of quasi-resonant oscillation. Thus, taking the monotonic decrease with increasing E_0 into consideration, we assume that the differential scattering cross section σ for $\theta = 90^\circ$ is proportional to the inverse of the *m*-th power of E_0, that is,

$$\sigma(E_0, \theta) = \sigma(E_0, 90^\circ) = \sigma \propto E_0^{-m} \quad . \tag{25}$$

By combining the above equation with eq. (24), we can write I as

$$\begin{aligned} &I \propto I' \\ &I' = \left[1 - n_{aa}(\infty)\right] E_0^{-m} \cdot \end{aligned} \tag{26}$$

Figure 6 show I' defined by eq. (26) as a function of the incident energy of the ion, E_0, schematically. Figure 7 shows the scattering ion yields of the He^+-Ga, He^+-Sn, He^+-In, and He^+-Cu systems experimentally determined by Rusch and Erickson[30]. Although theoretical calculations showed oscillations similar to those observed in the experimental data, most of the oscillations were observed at low energies, below approximately 100 eV, whereas the experimental data showed long-range oscillations beyond approximately 1500 eV, as illustrated in Fig. 7. Furthermore, the numerical calculations indicated that *I'* tends to decrease with oscillation over the entire range of

energy. In contrast, the experimentally determined intensity tended to increase with oscillation in the energy range below several hundreds of eV. Therefore, it seems that the theoretical model based on eqs. (4)-(6) (the localized *d* state model) can't sufficiently account for the experimental data regarding resonant or quasi-resonant neutralization processes.

Since the electronic configurations of Ga, Sn, and In are $[Ar]3d^{10}\ 4s^2 4p^1$, $[Kr]4d^{10}5s^2 5p^2$, and $[Kr]4d^{10}5s^2 5p^1$, the *d* electrons of Ga, Sn, and In may form band structures characterized by a narrow bandwidth and a relatively high density of states(DOS), like the 3*d* bands of the transition metals Fe, Co, and Ni. In contrast, the *s,p* electrons in the outer shells form a valence band in the vicinity of the Fermi level, which is characterized by a wide bandwidth and a relatively low DOS. Therefore, the theoretical model based on band electrons seems to be more suitable for explaining the experimental data. The improved model, which includes terms related to the presence of band electrons, is

$$\hat{H} = \hat{H}_0 + \hat{H}', \tag{27}$$

$$\hat{H}_0 = \sum_{\mathbf{k}} E_{\mathbf{k}} \hat{C}_{\mathbf{k}}^{+} \hat{C}_{\mathbf{k}} + E_a(z) \hat{C}_a^{+} \hat{C}_a , \tag{28}$$

$$\hat{H}' = \sum_{\mathbf{k}} (V_{a\mathbf{k}}(z) \hat{C}_a^{+} \hat{C}_{\mathbf{k}} + V_{\mathbf{k}a}(z) \hat{C}_{\mathbf{k}}^{+} \hat{C}_a); \tag{29}$$

thus, the corresponding quantum rate equations are

$$\frac{d}{dt} n_{aa}(t) = \frac{\mathrm{i}}{\hbar} \sum_{\mathbf{k}} V_{\mathbf{k}a}(t)\, n_{\mathbf{k}a}(t) - \frac{\mathrm{i}}{\hbar} \sum_{\mathbf{k}} V_{a\mathbf{k}}(t)\, n_{a\mathbf{k}}(t) , \tag{30}$$

$$\frac{d}{dt} n_{\mathbf{k}a}(t) = \frac{\mathrm{i}}{\hbar} (E_{\mathbf{k}} - E_a(z)) n_{\mathbf{k}a}(t) + \frac{\mathrm{i}}{\hbar} V_{a\mathbf{k}}(t) n_{aa}(t) - \frac{\mathrm{i}}{\hbar} \sum_{\mathbf{k}'} V_{a\mathbf{k}'}(t) n_{\mathbf{k}\mathbf{k}'}(t) , \tag{31}$$

$$\frac{d}{dt} n_{\mathbf{k}\mathbf{k}'}(t) = \frac{\mathrm{i}}{\hbar} (E_{\mathbf{k}} - E_{\mathbf{k}'}) n_{\mathbf{k}\mathbf{k}'}(t) + \frac{\mathrm{i}}{\hbar} V_{a\mathbf{k}}(t) n_{a\mathbf{k}'}(t) - \frac{\mathrm{i}}{\hbar} V_{\mathbf{k}'a}(t) n_{\mathbf{k}a}(t) . \tag{32}$$

Furthermore, altering the notation to use j, j' instead of the $\mathbf{k}, \mathbf{k}'$ used in eqs. (30)-(32) and simplifying $V_{aj}(t)$ as $V(t)$, with no dependence on *j*, we can rewrite the above equations as

$$\frac{d}{dt} n_{aa}(t) = \frac{\mathrm{i}}{\hbar} V(t) \left(\sum_{j=1}^{N} n_{ja}(t) - \frac{\mathrm{i}}{\hbar} \sum_{j=1}^{N} n_{aj}(t) \right), \tag{33}$$

$$\frac{d}{dt} n_{ja}(t) = \frac{\mathrm{i}}{\hbar} (E_j - E_a(z)) n_{ja}(t) + \frac{\mathrm{i}}{\hbar} V(t) (n_{aa}(t) - \sum_{j'=1}^{N} n_{jj'}(t)), \tag{34}$$

$$\frac{d}{dt} n_{jj'}(t) = \frac{\mathrm{i}}{\hbar} (E_j - E_{j'}) n_{jj'}(t) + \frac{\mathrm{i}}{\hbar} V(t) (n_{aj'}(t) - n_{ja}(t)). \tag{35}$$

When solving eqs. (33)-(35) numerically, we defined E_j as $E_j = E_{\text{center}}^{\text{band}} + \Delta E \cdot (\frac{N-1}{2} - j + 1) \, (j = 1, 2, \cdots, N)$, with $\Delta E = 40\text{meV}$. N is usually an odd number; thus, $E_j = E_{\text{center}}^{\text{band}}$ at $j = (N+1)/2$, i.e., the intermediate value of *N*; for example, $j = 11$ when *N* = 21. For the central energy of the band electrons $E_{\text{center}}^{\text{band}}$, we set $E_{\text{center}}^{\text{band}} = -20\text{eV}$, which is close to $-I (I = 24.58\text{eV}:$ first ionization potential of He$)$. Additionally, on the basis of the above definitions, the bandwidth D is given by $D = (N-1)\Delta E$. Concerning the initial conditions, we set $n_{aa}(-\infty) = 0, n_{ja}(-\infty) = 0, n_{jj'}(-\infty) = \delta_{jj'}$.

Figures 8(A), (B), and (C) show the evaluated $1 - n_{aa}(\infty)$ derived from the numerical calculations of eqs. (33)-(35) for *D* = 0.8, 1.6, and 2.4 eV, respectively. As illustrated in these figures, the values of $1 - n_{aa}(\infty)$ in the low-ion-velocity range tended to be smaller, which indicates that the He^+ ion can be easily neutralized at low incident energies. Although these figures show relatively small values of $1 - n_{aa}(\infty)$ at low incident energies, the range of neutralization tended to extend with increasing *D*. This extension of the neutralization range with *D* is therefore considered a result of the

interactions between the ion and many band electrons, mainly associated with D. Consequently, such small values of ISS data at low incident energies, as experimentally observed in Fig. 7, are probably considered a result of neutralization due to the effect of the band electrons.

Figures 9(A), (B), and (C) show I' as defined in eq.(26) for D = 0.8, 1.6, and 2.4 eV, respectively. Compared with the previous results shown in Fig. 6, the model including the effects of the band electrons seems to more accurately simulate the experimental data. Through comparison with Fig.7, especially in the case of N = 61, i.e., D = 2.4 eV, the calculated results shown in Fig. 9(C) are closer to the experimental data. The theoretically evaluated period of oscillation was greatly reduced, to about 0.008 $eV^{-1/2}$ in comparison with the previous result of 0.06 $eV^{-1/2}$. This marked decrease can be ascribed to the extension of the oscillation range beyond 1000 eV, which was caused by the band electrons.

Certainly the quantitative agreement between Fig. 9(C) and the experimental data (Fig.7) is not very good, but such small values, experimentally observed at low incident energies, as shown in Fig. 7, are numerically simulated in Fig. 9(C), which was impossible using the model based on eqs. (4)-(6) (localized d state model). Furthermore, it should be noted that the peaks of I', usually observed at incident energies higher than 1000 eV, which the localized d model and band models with D = 0.8 and 1.6 eV cannot express numerically, were clearly observed in Fig. 9(C) (case of D = 2.4 eV), even though the theoretically evaluated peak positions were different from the experimentally observed ones. The quantitative disagreements were mainly due to the bandwidth D and the surface-ion interaction $V(t)$. Therefore, the quantitative mismatch should be improved by substituting more

precise parameter values. However, interpretation on the basis of the band model does seem to qualitatively explain the experimental data.

4. Conclusions

We have theoretically examined quasi-resonant and resonant neutralization processes, such as those observed in the He^+-Ga, He^+-Sn, and He^+-In systems, using quantum rate equations. The calculated ISP as a function of inverse ion velocity v was found to oscillate with a constant period, as has been experimentally observed in the He^+-Ga, He^+-Sn, and He^+-In systems. Furthermore, on the basis of the 2nd-order differential equation (eq. (22)) derived from the quantum rate equations, we obtained analytical results consistent with those previously calculated using other theoretical approaches (such as the time development operator method)[51].

We attempted to apply the present method to the analysis of quasi-resonant and resonant neutralization processes. After assuming that the *d*-level of the target atom has only one energy level, E_d, with no formation of a band structure (localized *d* state model), we examined these quasi-resonant systems numerically and theoretically, and then compared the results with available experimental data. The results calculated on the basis of the localized *d* state model showed oscillations, as were observed experimentally. However, most of the oscillations were found in a small range of incident energies below 500 eV, while the experimental data showed oscillations even at incident energies above 1400 eV. Furthermore, the localized model could not numerically simulate or reproduce the relatively small values of the ISS spectra at low incident energies below 600 eV, as were

experimentally observed in the He^+-Ga, He^+-Sn, and He^+-In systems. The quantitative agreement was unacceptable.

To improve the agreement between the theory and the experiment, we proposed an alternative model (band model), in which incident He^+ ions are scattered by the many band electrons existing on the surface and are neutralized as a result of electron transfer from the band electrons. The mismatch was much improved, and ISS data similar to experimental observations were obtained. In particular, when the bandwidth *D* was as wide as 2.4 eV, relatively small values were observed in the spectra at low incident energies, which the localized *d* state model could not account for. Consequently, our proposed band model is suitable for the analysis of quasi-resonant or resonant neutralization processes, and the effect of band electrons plays a very important role in determining neutralization processes. Furthermore, it should be noted that the behavior of spectra in the low-incident-energy region is strongly affected by the bandwidth *D*.

The proposed model can explain the experimental data qualitatively. However, the numerical agreement between the theoretical and experimental data remains incomplete. To decrease the numerical mismatch and simulate experiments more precisely, we should consider the following points.

4.1 More detailed description of the energy dispersion of the band structure

In this article, in order to perform smooth calculations and reduce computation time, we defined the band structure (energy dispersion) in a simplified form as

$$E_j = E_{\text{center}}^{\text{band}} + \Delta E \cdot (\frac{N-1}{2} - j + 1)\,(j = 1,2,\cdots,N)\,.$$

The above expression corresponds to DOS = ρ_0(const) within a finite bandwidth D . An actual metal surface is much more complex, so calculations including a more detailed energy dispersion, i.e., DOS, would provide quantitative improvement. Concerning the numerical scheme for expressing the DOS, we can consider the equation below to determine $\{E_j\}$:

$$\int_{E_j}^{E_{j+1}} \rho(E)dE \cong \frac{1}{2}(E_{j+1} - E_j)(\rho(E_j) + \rho(E_{j+1})) = \Delta n_0\,,$$

where $\rho(E)$ is the DOS for 3*d*-or 4*d* band electrons of surface and Δn_0 is a positive arbitrary constant with no dimension. By solving the above equation numerically, we can obtain $\{E_j\}$ corresponding to $\rho(E)$; thus, it is possible to carry out the calculation including the DOS of more complex energy dispersion.

4.2 Determination of more precise $V(t)$

We used $V(t)$ instead of $V_{a\mathbf{k}}(t)$ in this study, ignoring the difference in interaction between the He^+ ion and an electron with a momentum ***k***. This approximation was too crude to simulate the system accurately. In further calculations to determine a more precise $V_{a\mathbf{k}}(t)$, we should consider and evaluate the precise interaction between the He^+ ion and the surface.

4.3 Closer description of $E_a(z)$

Usually, the energy level of a vacant ion level tends to increase as the ion approaches a surface,

because of Pauli's exclusion principle. In this study, we analyzed resonant and quasi-resonant systems using eq. (21). However, eq. (21) was too simple to simulate the resonant or quasi-resonant behavior quantitatively. Therefore, a more detailed, experimentally determined formula should be applied to improve the simulations.

4.4 Auger neutralization

In this study, we did not introduce the Auger neutralization process. Certainly, the Auger neutralization process is considered to be important, at least, at low incident energies. Therefore, we can't refute the hypothesis that the observed ISS data can mainly be attributed to Auger neutralization. However, as illustrated in Fig. 7, ISS experiments related to the He^+-Sn, He^+-In, and He^+-Ga systems showed several slight peaks at incident energies below 400 eV. Therefore, the contribution of resonant and quasi-resonant neutralization processes should be taken into account. Further detailed investigation of both neutralization processes is required.

The above four points are considered essential to the qualitative fitting and analysis of the experimental data using a theoretical model.

The quantum rate equations conclusively showed good agreement with previous experimental and theoretical results. These equations can explain the resonant or quasi-resonant system from a qualitative viewpoint and show that the behavior of spectra at relatively low incident energies is strongly affected by the bandwidth D. To understand and interpret experimental data theoretically, further study to improve the above four points is needed, with emphasis on the effect of the many

surface electrons.

References

1) D. P. Smith: Surf. Sci. **25** (1971) 171.

2) W. Heiland and E.Taglauer: Nucl. Instrum. Methods **132** (1976) 535.

3)H. Niehus: in *Ion and Neutral Spectroscopy, Practical Surface Analysis*, ed. D. Briggs and M. P. Seah (Wiley, Chichester, 1992) Vol. 2, Chap. 9.

4) H. Niehus, W. Heiland and E. Taglauer: Surf. Sci. Rep. **17** (1993) 213.

5)R. S. Williams: in *Low-Energy Ion Surface Interactions*, ed. J.W. Rabalais (Wiley, Chichester, 1994) Chap. 1.

6)S. H. Overbury: in *Handbook of Surface Imaging and Visualization*, ed. A. T. Hubbard(CRC, Boca Raton, 1995) Chap. 26.

7)E.Taglauer: in *Surface Analysis-The Principal Techniques*, ed. J.C. Vickerman(Wiley, Chichester, 1997) Chap. 6.

8) A. Benninghoven: Z. Phys. **199** (1967) 141.

9) V. Matolin, E. Gillet, N. M. Reed, and J. C. Vickerman: J. Chem. Soc. Faraday Trans.**86** (1990) 2749.

10) P. D. Prewett and G. L. R. Mair: in *Focused Ion Beams from Liquid Metal Ion Sources*(Research Studies Press, Taunton,1991).

11) R. M. Braun, P. Blenkinsopp, S. J. Mullock, C. Corlett, K. F. Willey, J. C. Vickerman, and N.Winograd: Rapid Commun.Mass Spectrom. **12** (1998) 1246.

12) B.Cliff, N. Lockyer, H. Jüngnickel, G.. Stephens,and J.C.Vickerman: Rapid Commun. Mass

Spectrom. **17** (2003) 2163.

13) D. Menzel and R. Gomer: J. Chem. Phys.**41** (1964) 3311.

14) P. A. Redhead: Can. J. Phys.**42** (1964) 886.

15) P. J. Feibelman and M. L. Knotek: Phys.Rev.V, **18** (1978) 6531.

16) P.Antoniewicz: Phys. Rev.B.**21** (1980) 3811.

17) W.Brenig: in *Desorption Induced by Electron Transitions*, ed. N.H.Tolk, M.M.Traum, J.C.Tully and T.E.Madey (Springer, Berlin, 1983) Vol.24, p.90.

18) M.L.Knotek: Rep.Prog.Phys.**47** (1984) 1499.

19) H. D. Hagstrum: Phys.Rev. **96** (1954) 336.

20) H. D. Hagstrum: Phys.Rev. **122** (1961) 83.

21) H. D. Hagstrum: in *Electron and ion Spectroscopy of Solids*, ed. L.Fiermans(Plenum Press, New York, 1978) p.273.

22) H. D. Hagstrum: in *Chemistry and Physics of Solid Surfaces VII*, ed. R.Vanselow and R.F.Howe (Springer, Berlin, 1988) Vol. 10, p.341.

23) D. P. Woodruff: Nucl.Instrum.Methods. **B194** (1982) 639.

24) R.Kumar, M.H.Mintz, J.A.Schultz, and J.W.Rabalais: Surf.Sci.**130** (1983) L311.

25) R.Cortenraad, A.W.D.van der Gon, H.H.Brongersma, S.N.Ermolov, and V.G.Glebovsky: Phys.Rev. B **65** (2002) 195414.

26) A.Kutana, M.J.Gordon, and K.P.Giapis: Nucl.Instrum.Methods. **B 248** (2006) 16.

27) R.L.Erickson and D.P.Smith: Phys.Rev.Lett.**34** (1975) 297.

28) N.H.Tolk ,J.C.Tully, J.Kraus, C.W.White, and S.N.Neff: Phys.Rev.Lett.**36** (1976) 747.

29) J.C.Tully and N.H.Tolk: in *Inelastic Ion-surface Collisions*, ed. N.H.Tolk(Academic, NewYork,1977).

30) T.W.Rusch and R.L.Erickson: J.Vac.Sci.Technol. **13** (1978) 374.

31) A.Zartner, E.Taglauer and W.Heiland: Phys.Rev.Lett. **40** (1978) 1259.

32) W.L.Baun: Surf.Sci. **100** (1980) L491.

33) D.J.O'Connor and R.Beardwood: Nucl.Instrum.Methods. **B48** (1990) 358.

34)A.D.F.Kahn, D.J.O'Connor, and R.J.MacDonald: Surf.Sci. Lett.**262** (1992) L83.

35) O.S.Oen and M.T.Robinson: Nucl.Instrum.Methods. **132** (1976) 647.

36) J.C.Tully: Phys.Rev.B.**16** (1977) 4324.

37) S.I.Easa and A.Modinos: Surf.Sci. **161** (1985) 129.

38) N.Vitanov and G.. Panev: J.Phys.B:At.Mol.Opt. Phys. **25** (1992)239.

39) L.V.Keldysh: Sov.Phys.JETP. **20** (1965) 1018.

40) T.Sakai, M.Sakaue, H.Kasai, and A.Okiji: Appl.Surf.Sci. **169-170** (2001) 57.

41) E.A.GarÍa, C.G..Pascual, P.G..Bolcatto, M.C.G.Passeggi, and E.C.Goldberg: Surf.Sci. **600** (2006) 2195.

42) M.Krawiec, M.Jałochowski, and M.Kisiel: Surf.Sci. **600** (2006) 1641.

43) S.Kondo and K.Yamada: Prog.Theor.Phys. **122** (2009) 713.

44) R.Brako and D.M.Newns: Surf.Sci.**108** (1981) 253.

45) L.Landau: Z.Phys.Sowjet. **2** (1932) 46.

46) C.Zener: Proc.Roy.Soc.(London) **A137** (1932) 696.

47) E.C.G.Stueckelberg: Helv.Phys..Acta **5** (1932) 369.

48) V.K.Bykhovskii, E.E.Nikitin, and M.Ya.Ovchinnikova: Soviet Phys.-JETP **20** (1965) 500.

49) M.Cardona and L.Ley: in *Photoemission in Solids* I (Springer,NewYork,1978).

50) J.A.Bearden and A.F.Burr: in *X-ray Wavelengths and X-ray Atomic Energy Levels* (Washington, DC, 1967) NSRDS-NBS 14,US GPO.

51) S.Tsuneyuki, N.Shima, and M.Tsukada: Surf. Sci. **186** (1987) 26.

52) E.Taglauer and W.Heiland: Surf.Sci.**47** (1975) 234.

53) E.Everhart, G.Stone, and R.J.Carbone: Phys.Rev. **99** (1955) 1287.

54) M.T.Robinson: Oak Ridge National Laboratory Report, (1963) ORNL-3943.

Figure captions

Fig. 1. Dependence of ISP on time, where we set ion-surface interaction $V(t) = V_0 \exp(-\zeta v^2 t^2)$ (v: ion velocity, ζ: positive constant, t: time) and V_0, ζ and v are 1.2 eV, 1.0 Å^{-2} and 15 km/s, respectively.

Fig. 2. Dependence of ISP on the velocity of ion, where ion-surface interaction is the same as in Fig. 1.

Fig. 3. Calculated relation between ISP and ion velocity v at work functions ϕ=1, 3 and 5 eV, where ion-surface interaction is the same as in Fig.1, binding energy of target atom=20 eV and ionization potential=24.58 eV.

Fig. 4. Relation of ion-surface distance *z* and energy level of ion E_a on the basis of eq. (21), where we take -2 a_B as the value of the location of image potential (a_B: Bohr radius)

Fig. 5. Plot of the ISP in Fig. 3 for ϕ=3 eV as a function of inverse of ion velocity v.

Fig. 6. Schematic illustration of *I'* as defined in eq. (26) based on the numerical calculation results of eqs. (9)-(11), where ion-surface interaction is the same as in Fig.1, binding energy of target atom=20eV ,ionization potential=24.58 eV, work function ϕ=3 eV and m =1/2.

Fig. 7. Experimentally determined scattering ion yields of He^+-Ga, He^+-Sn, He^+-In and He^+-Cu systems by Rusch and Erickson[30].

Fig. 8. Evaluated $1 - n_{aa}(\infty)$ derived from the numerical calculations using eqs. (33)-(35) for various bandwidths D where (A) D = 0.8 eV (B) D = 1.6 eV (C) D = 2.4 eV. The ion-surface interaction is the same as in Fig.1, binding energy of target atom=20 eV,

ionization potential=24.58 eV and work function ϕ=3 eV.

Fig. 9. Schematic illustration of I' as defined in eq.(26) on the basis of the numerical calculation results obtained using eqs. (33)-(35) for various bandwidths D where (A) D = 0.8 eV (B) D = 1.6 eV (C) D = 2.4 eV. The ion-surface interaction is the same as in Fig.1, binding energy of target atom=20 eV ionization potential=24.58 eV, work function ϕ=3 eV and m=1/2.

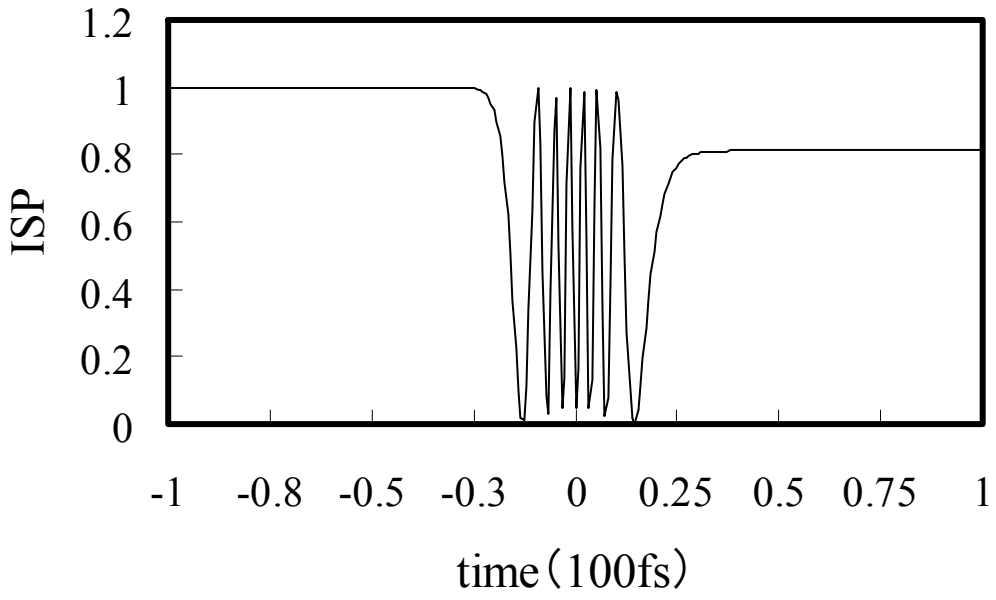

Fig.1

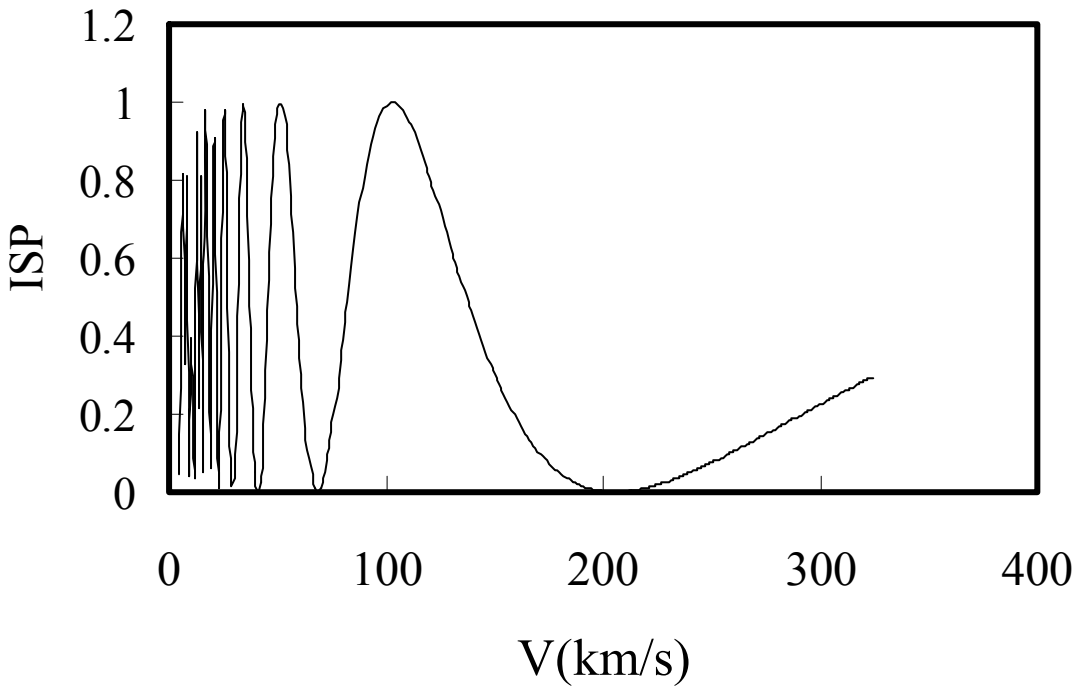

Fig.2

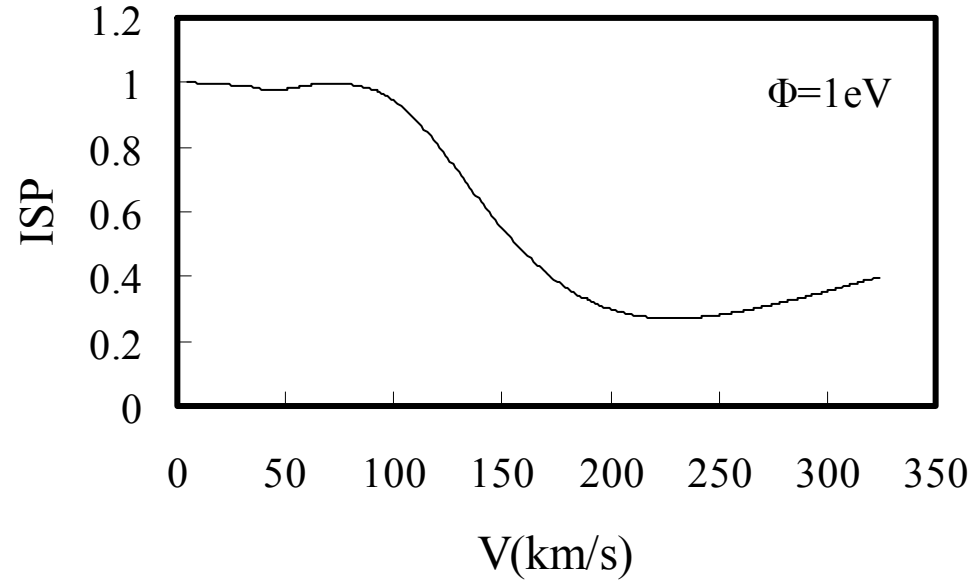
1.2
1
0.8
0.6
0.4
0.2
0
ISP
Φ=1eV
0
50
100
150
200
250
300
350
V(km/s)

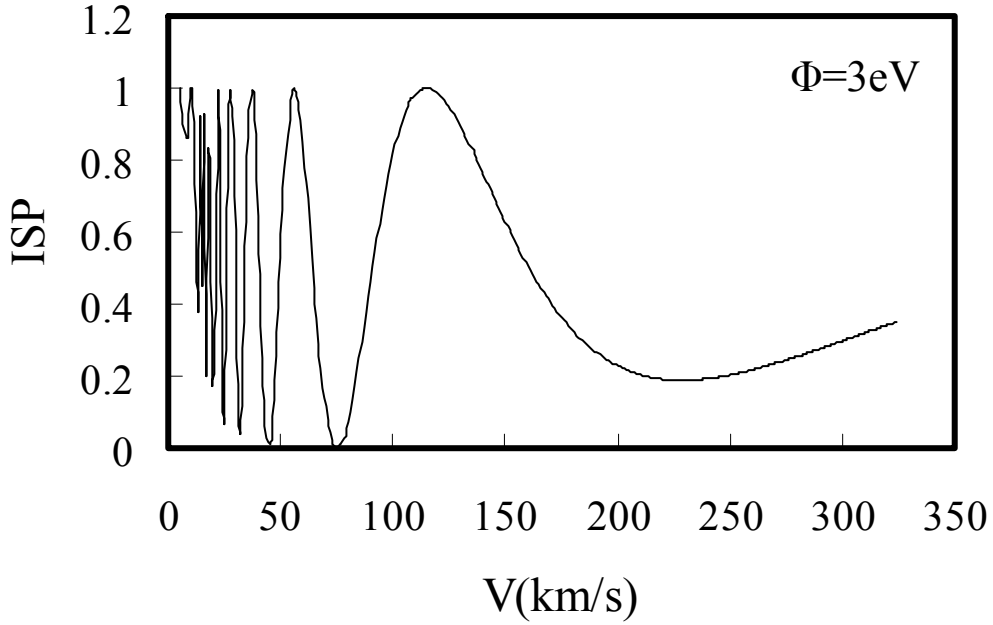
1.2
1
0.8
0.6
0.4
0.2
0
ISP
Φ=3eV
0
50
100
150
200
250
300
350
V(km/s)

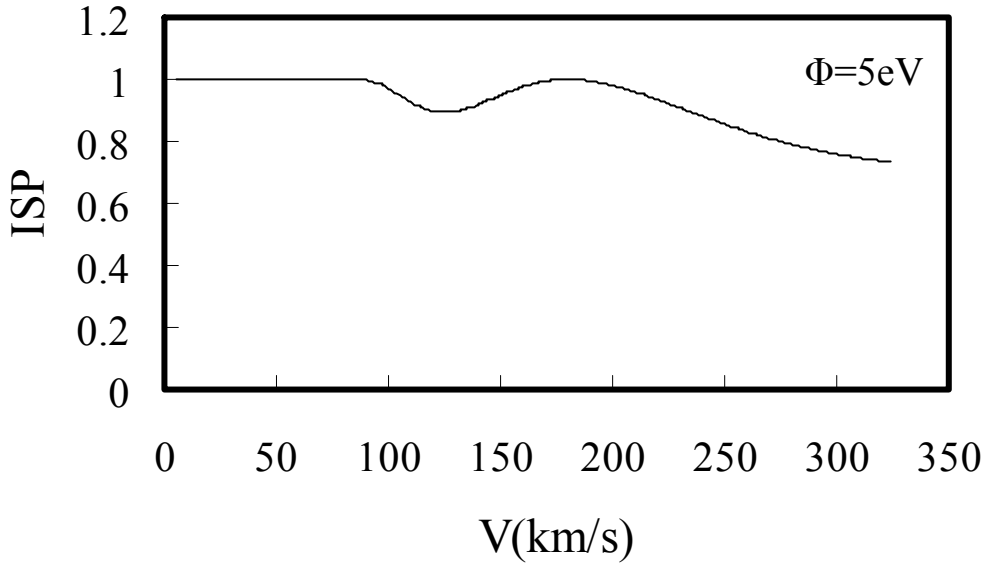
1.2
1
0.8
0.6
0.4
0.2
0
ISP
Φ=5eV
0
50
100
150
200
250
300
350
V(km/s)

Fig.3 35

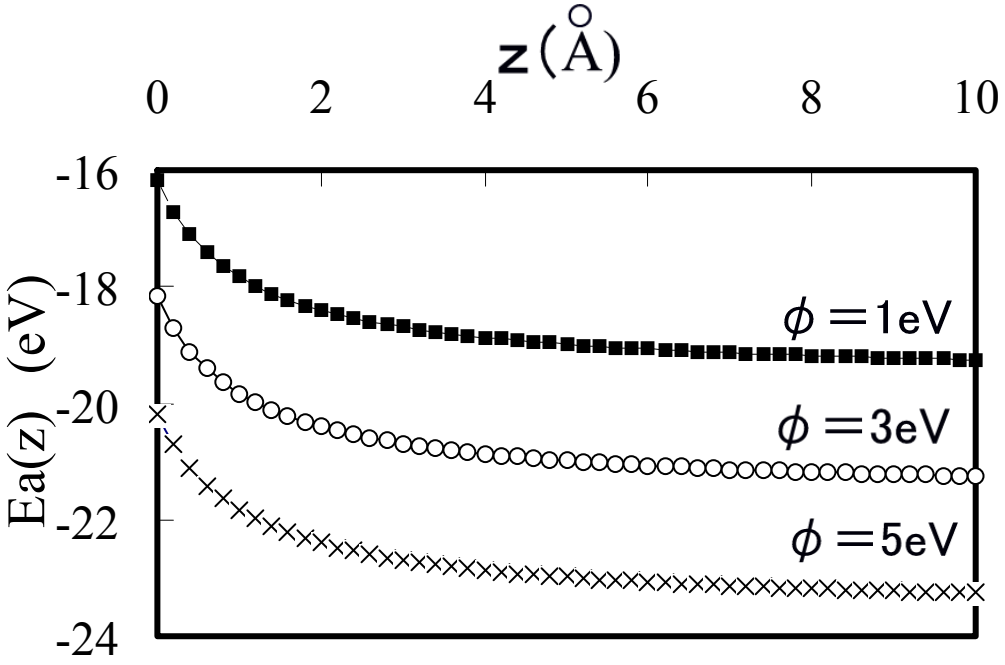

Fig.4

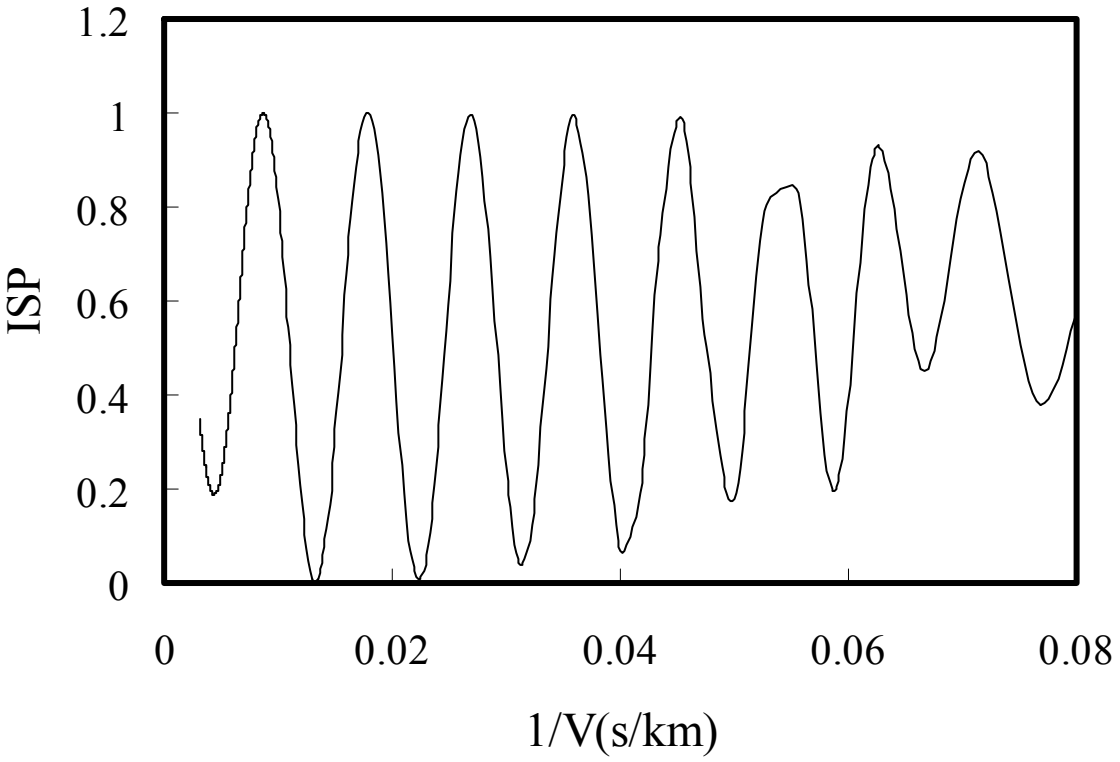

Fig.5

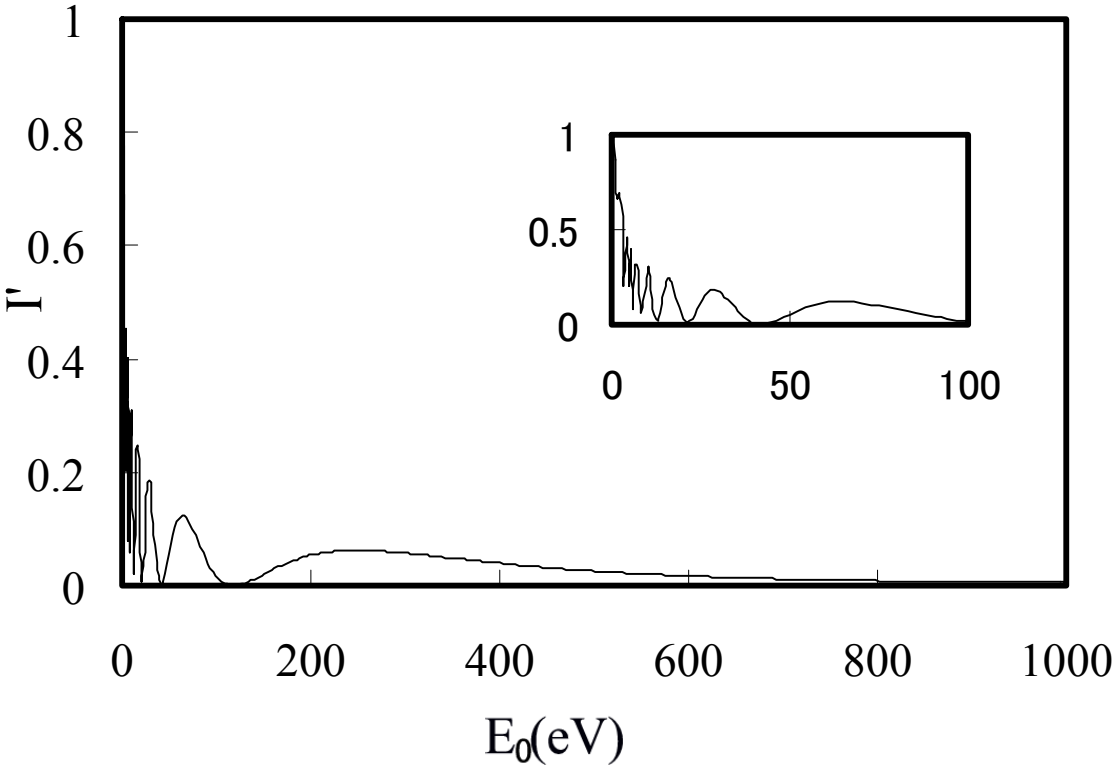

Fig.6

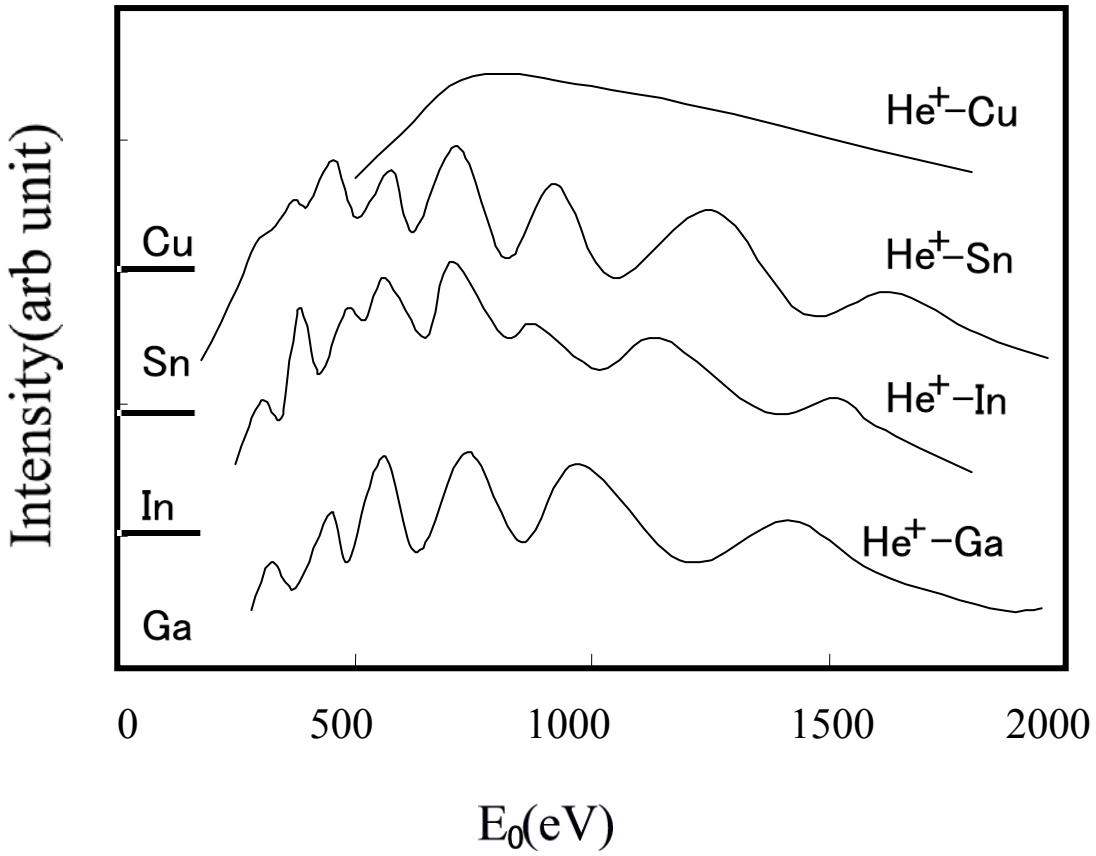
Intensity(arb unit)
Cu
Sn
In
Ga
He+–Cu
He+–Sn
He+–In
He+–Ga
0
500
1000
1500
2000
E0(eV)

Fig.7

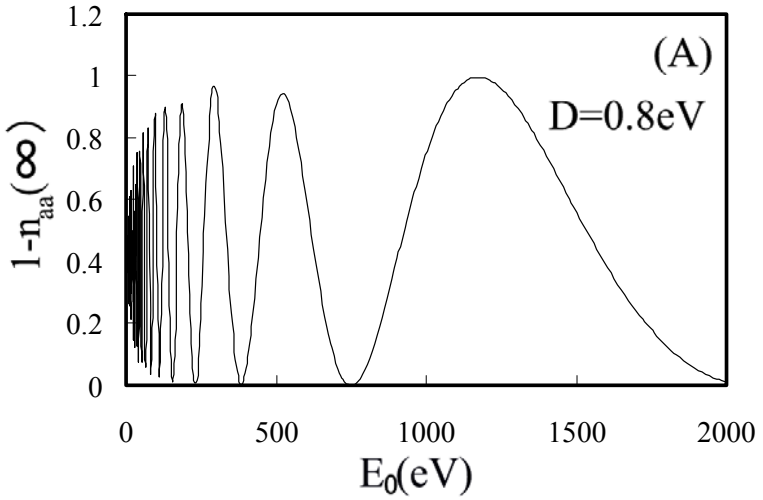

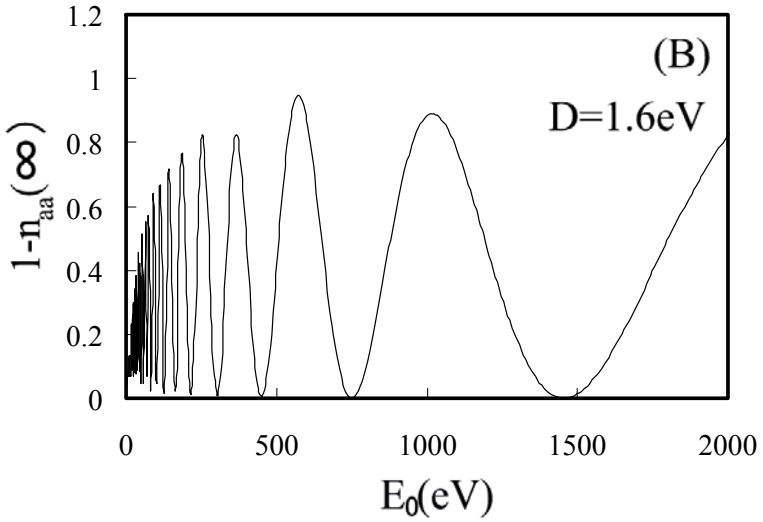

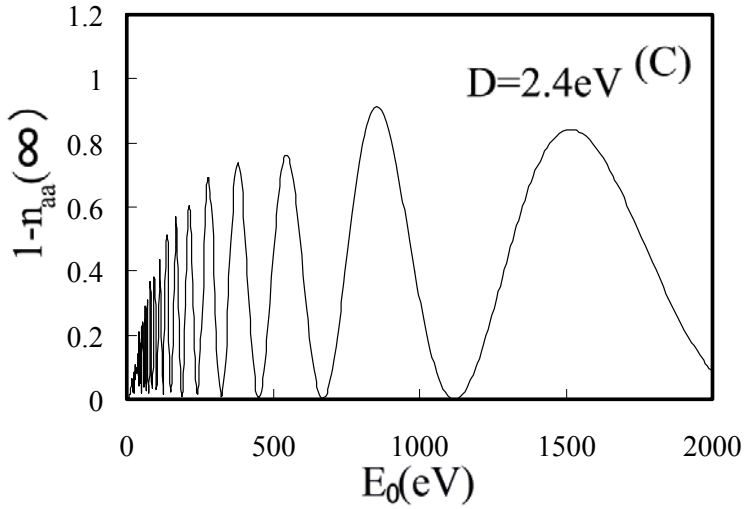

Fig.8

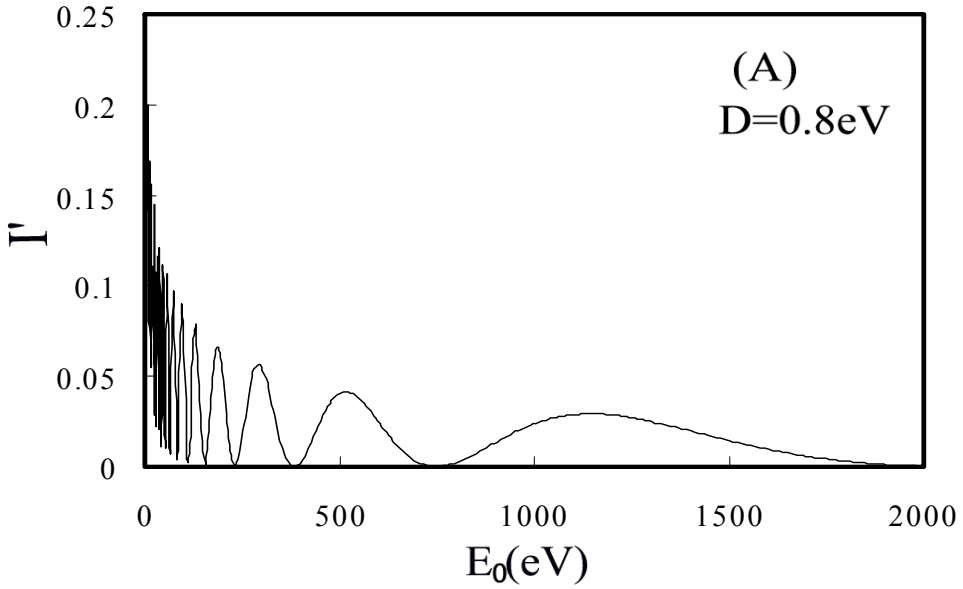
(A)
D=0.8eV
I'
0.25
0.2
0.15
0.1
0.05
0
0
500
1000
1500
2000
E0(eV)

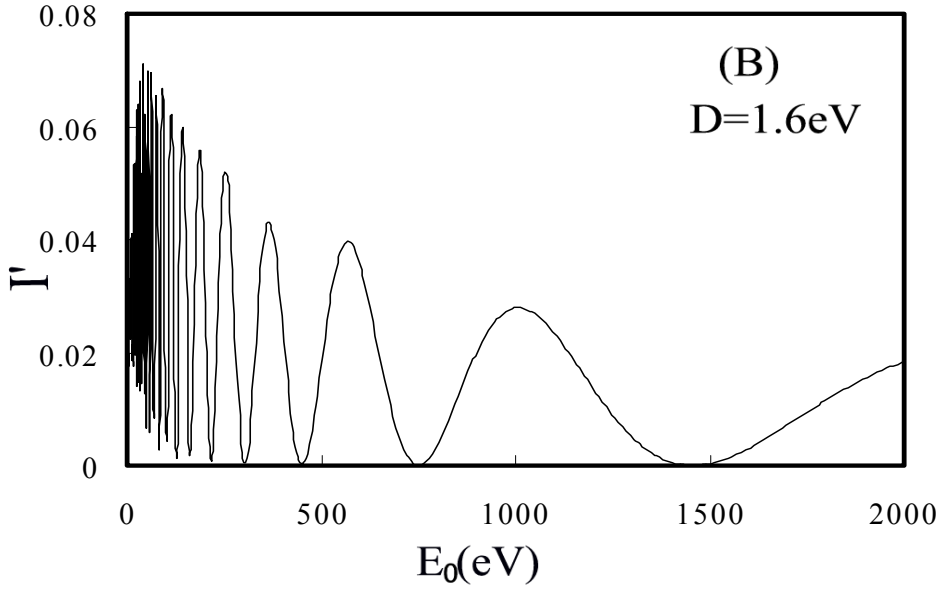
(B)
D=1.6eV
I'
0.08
0.06
0.04
0.02
0
0
500
1000
1500
2000
E0(eV)

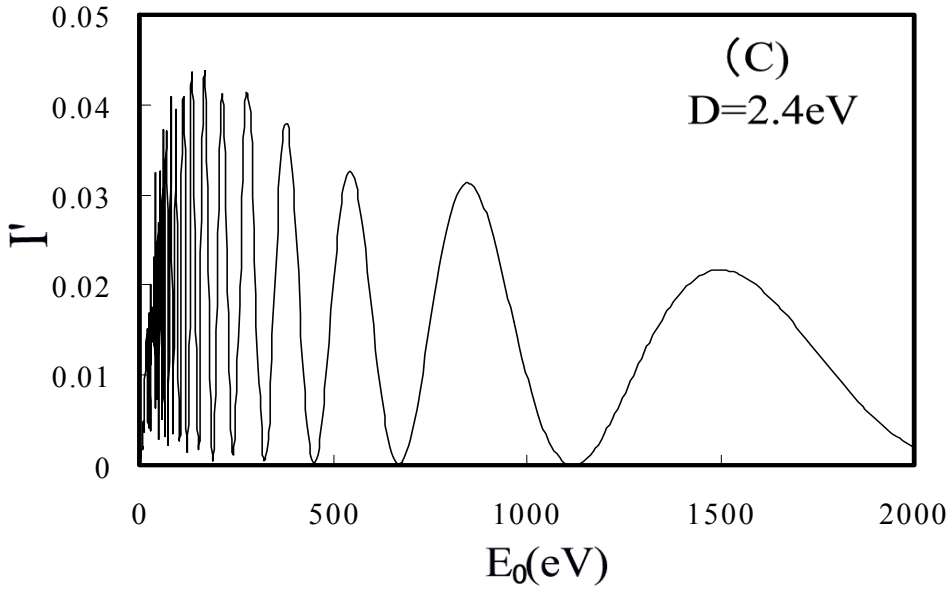
(C)
D=2.4eV
I'
0.05
0.04
0.03
0.02
0.01
0
0
500
1000
1500
2000
E0(eV)

Fig.9